INTERNATIONAL JOURNAL OF HYDROGEN ENERGY 42 (2017) 22496–22501

Available online at www.sciencedirect.com

ScienceDirect

journal homepage: www.elsevier.com/locate/he

Computational study of the vibrational spectroscopy properties of boron-hydrogen compounds: $Mg(B_3H_8)_2$, $CB_9H_{10}^-$ and $CB_{11}H_{12}^-$

Daniel Sethio, Latévi Max Lawson Daku, Hans Hagemann***

Faculty of Sciences — University of Geneva, Quai Ernest Ansermet 30, 1211 Geneva, Switzerland

ARTICLE INFO

Article history:
Received 13 January 2017
Received in revised form
1 March 2017
Accepted 8 March 2017
Available online 31 March 2017

Keywords:
Boron-hydrogen species
IR
Raman
Vibrational frequencies
Anharmonicity
Density functional theory

ABSTRACT

We report the DFT study of the vibrational spectroscopy properties of $Mg(B_3H_8)_2$, a potential intermediate in the decomposition of $Mg(BH_4)_2$, as well as those of $CB_{11}H_{12}^-$ and $CB_9H_{10}^-$, whose salts can exhibit high ionic conductivities. Because the inclusion of anharmonicity is key to the accurate description of the vibrational properties of BH species [D. Sethio, L. M. Lawson Daku, H. Hagemann. Int. J. Hydrogen Energy, 41 (2016) 6814], the calculations were performed both in the harmonic and in the anharmonic approximation. The IR and Raman spectra of $Cs(CB_{11}H_{12})$ and $Na_2(B_{10}H_{10})$ have also been measured. The calculated and experimental spectra are in good agreement. A comparative analysis of the vibrational spectroscopy properties is made for $B_3H_8^-$ and $Mg(B_3H_8)_2$, $B_{12}H_{12}^{2-}$ and $CB_{11}H_{12}^-$, and for $B_{10}H_{10}^{2-}$ and $CB_9H_{10}^-$.

Introduction

Boron-hydrogen compounds are receiving a lot of attention for very various reasons. Thus, $Mg(B_3H_8)_2$ and $MgB_{12}H_{12}$ are potential intermediates in the decomposition of $Mg(BH_4)_2$ [1–8]. On an unrelated note, $Na(CB_{11}H_{12})$, $Na(CB_9H_{10})$ and mixture of both show remarkably high ionic conductivities and stabilities, which make them suitable for use in rechargeable battery application [9–12].

Previous studies have examined the structures, reactivity, the relative stabilities and spectroscopic properties of boron-hydrogen species; see, for instance [13–26], and references therein. Vibrational spectroscopy is a powerful method to characterize the structure and dynamics of molecular systems. For the boron-hydrogen species, the inclusion of anharmonicity proves to be key for the accurate prediction of their IR and Raman spectra [27].

In this work, we calculate the IR and Raman spectra of $Mg(B_3H_8)_2$ and compare them to those of the free $B_3H_8^-$ ion to assess the influence of the complexation to Mg^{2+}. Similarly, we investigate the differences observed between the IR and Raman spectra of $B_nH_n^{2-}$ and $CB_{n-1}H_n^-$ ($n = 10$ and $n = 12$) in order to probe the influence of the symmetry breaking induced by the B → C chemical substitution in closoborane cages. For all calculations, anharmonic effects are included. We have also measured the IR and Raman spectra of $Cs(CB_{11}H_{12})$ and $Na_2(B_{10}H_{10})$.

* *Corresponding author.*
** *Corresponding author.*
E-mail addresses: max.lawson@unige.ch (L.M. Lawson Daku), hans-rudolf.hagemann@unige.ch (H. Hagemann).
http://dx.doi.org/10.1016/j.ijhydene.2017.03.044

Methods

Computational details

All calculations were performed with the Gaussian09 program package [28], using the procedure reported in Ref. [27] for an accurate prediction of the vibrational species of boron-hydrogen species. Thus, the B3LYP functional [29,30] augmented with Grimme's D2 [31] dispersion correction was employed in combination with the large correlation-consistent cc-pVTZ basis. The geometries were optimized using an “ultra-fine” grid and “tight” convergence criteria for the forces and displacements. Vibrational frequencies analyses were then conducted both in the harmonic and in the anharmonic approximation using second-order perturbation theory as implemented in Gaussian09 [32–34].

Experimental details

$Cs(CB_{11}H_{12})$ was purchased from Katchem and used without any further purification. The FTIR spectrum was measured using a Biorad Excalibur Instrument equipped with a Specac Golden Gate heatable ATR setup at room temperature. The spectral resolution was set to 1 cm^{-1}. Raman spectrum was recorded using 488 nm excitation and a Kaiser Optical Holospec monochromator equipped with a liquid nitrogen cooled CCD camera.

Results and discussion

$B_3H_8^-$ is a fluxional ion which is formed as an intermediate during the reversible dehydrogenation of $Mg(BH_4)_2$ and $Y(BH_4)_3$ [35–37]. The interconversion between its possible different forms occurs by hydrogen migration [38]. In this study, we consider the most stable conformer of $B_3H_8^-$ and compare its vibrational properties to those of the complex $Mg(B_3H_8)_2$.

Fig. 1 shows the most stable conformer of $B_3H_8^-$ as well as $Mg(B_3H_8)_2$. $B_3H_8^-$ in its most stable form is of C_{2v} symmetry and has two B-H-B bridges (Fig. 1a). This form is preserved for the $B_3H_8^-$ moities of the complex $Mg(B_3H_8)_2$, which is of C_{2h} molecular symmetry. However, due to the coordination to Mg^{2+}, the B–H bond lengths for the outer H atoms (H_o) are shorter (1.185–1.188 Å) than those involving the inner (H_i) and bridging (H_b) hydrogen atoms (B–H_i = 1.223–1.229 Å, B–H_b = 1.255–1.469 Å). Fig. 2 compares the calculated IR and Raman spectra of $Mg(B_3H_8)_2$ with those of $B_3H_8^-$, which we previously reported [27].

Upon coordination to Mg^{2+}, the B–H_t (H_t: terminal H atoms) stretching modes of $B_3H_8^-$ around 2500 cm^{-1} are split into B–H_o and B–H_i stretching modes. The frequencies of the B–H_o stretching modes are larger than those of the B–H_i stretching modes. The B–H_o stretching modes are found around 2550 cm^{-1}, while the B–H_i stretching modes are found between 2200 cm^{-1} and 2300 cm^{-1}. One also notes that the B–H_b stretching modes have lower frequencies than the B–H_o and B–H_i stretching modes: these modes are indeed found around 2150 cm^{-1}. Table 1 summarizes the lengths and the associated anharmonic stretching frequencies of the different types of B–H bonds found in $B_3H_8^-$ and in $Mg(B_3H_8)_2$. Its inspection shows that the B–H bond lengths and stretching frequencies in $B_3H_8^-$ are both significantly influenced by the coordination to Mg^{2+}, and that the stretching frequency is larger the shorter the B–H bond. This observed correlation provides us with a

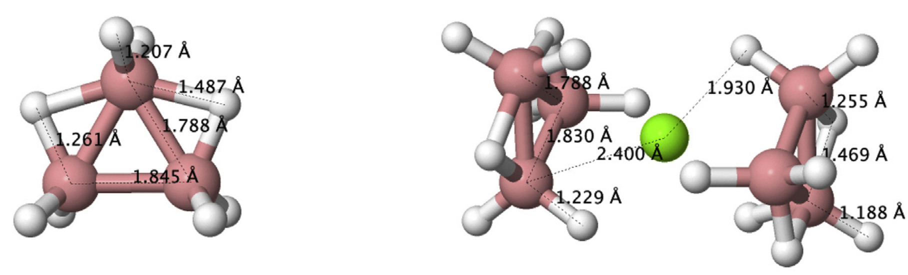

Fig. 1 – The most stable conformer of $B_3H_8^-$ ion (a) and the complex $Mg(B_3H_8)_2$ (b).

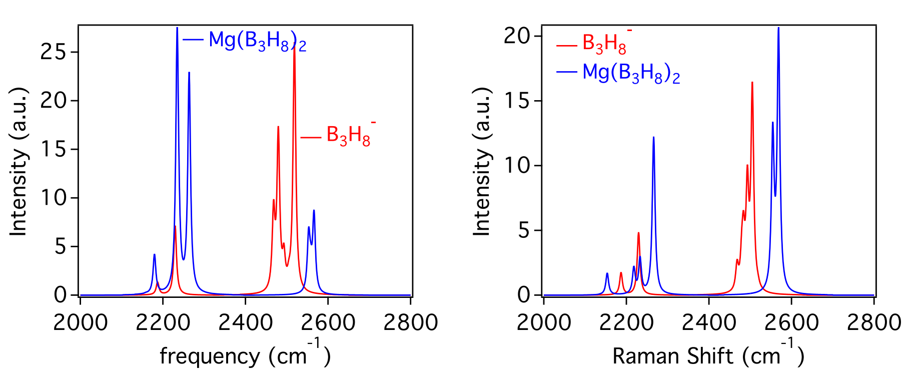

Fig. 2 – Calculated anharmonic IR (left) and Raman (right) spectra of $B_3H_8^-$ [27] and $Mg(B_3H_8)_2$.

Table 1 – The B–H bond lengths and the associated anharmonic stretching frequencies for $B_3H_8^-$ and $Mg(B_3H_8)_2$ (B3LYP-D2/cc-pVTZ results).

	$B_3H_8^-$ [a]	
	r (Å)	ν(cm^{-1})
B–H$_t$	1.207	2367–2399
B–H$_b$	1.261–1.487	2058–2131
	$Mg(B_3H_8)_2$	
	r (Å)	ν(cm^{-1})
B–H$_o$	1.185–1.188	2553–2568
B–H$_i$	1.223–1.229	2218–2266
B–H$_b$	1.255–1.469	2153–2180

[a] Ref. [27].

very good starting point for establishing a quantitative vibrational spectra–structure relations for $B_3H_8^-$–containing molecular species or compounds. Finally, in contrast to the vibrational spectra of $B_3H_8^-$, those of $Mg(B_3H_8)_2$ show some additional weak bands below 400 cm^{-1} (see Supporting Information), which are associated to complex motions that can be viewed as combinations of B–H, B–Mg, and B–B bending modes.

Salts of $CB_{11}H_{12}^-$, $B_{12}H_{12}^{2-}$, $CB_9H_{10}^-$, and $B_{10}H_{10}^{2-}$ ions attract much interest due to their high ionic conductivities. Fig. 3 compares the calculated anharmonic Raman spectrum of the isolated $CB_{11}H_{12}^-$ ion with the experimental Raman spectrum of $CB_{11}H_{12}^-$ in $Cs(CB_{11}H_{12})$ (left), as well as the experimental Raman spectra of $CB_{11}H_{12}^-$ and $B_{12}H_{12}^{2-}$ (right). The agreement between the calculated and experimental Raman spectra of $CB_{11}H_{12}^-$ is very satisfactory for both bending (Fig. 3) and stretching modes (see Supporting Information). On going from $B_{12}H_{12}^{2-}$ to $CB_{11}H_{12}^-$, the symmetry is lowered from I_h to C_{5v}: the IR active modes are split from T_{1u} to $A_1 + E_1$ and the Raman active modes transforming as H_g become $A_1 + E_1 + E_2$ in C_{5v}. These splittings appear clearly in the calculated spectra for the B–H bending and stretching modes at *ca.* 1000 cm^{-1} and at *ca.* 2500 cm^{-1}, respectively.

In order to illustrate the importance of including anharmonicity in the vibrational analyses of BH species, we compare in Fig. 4 the experimental Raman and IR spectra of $Cs(CB_{11}H_{12})$ with the calculated harmonic and anharmonic

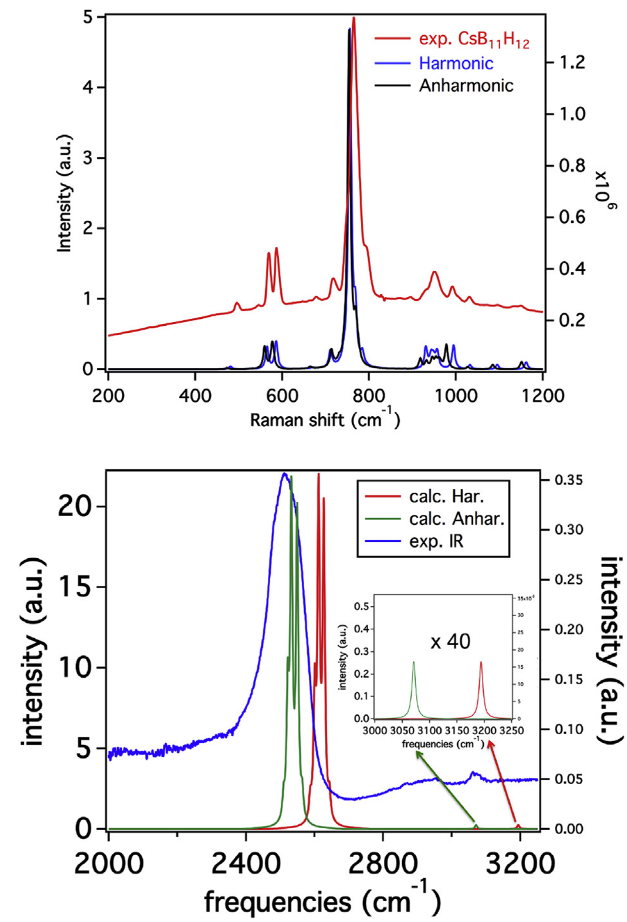

Fig. 4 – Comparison of the experimental Raman (Top) and IR (Bottom) spectra $Cs(CB_{11}H_{12})$ with the calculated harmonic and anharmonic Raman (Top) and IR (Bottom) spectra of $CB_{11}H_{12}^-$.

ones of $CB_{11}H_{12}^-$. In the bending mode region below 1200 cm^{-1}, the harmonic Raman spectrum already shows a satisfactory agreement with experiments, the inclusion of anharmonicity bringing small though noticeable changes to the predicted spectrum. The IR spectra are plotted between 2000 cm^{-1} and 3250 cm^{-1} in the stretching mode region. In

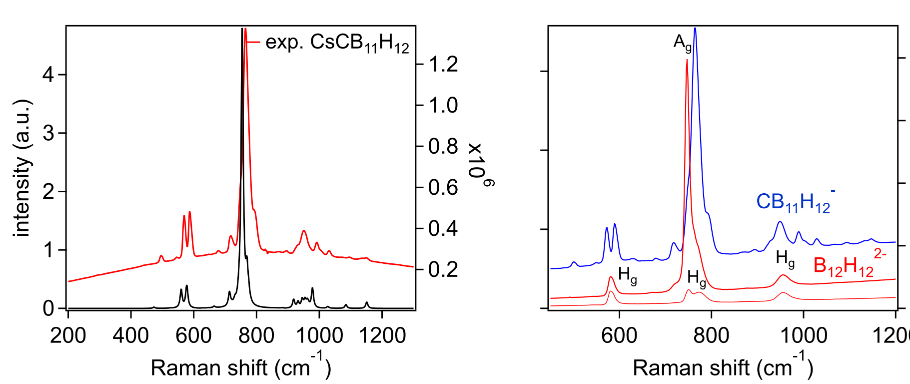

Fig. 3 – Comparison of the calculated anharmonic Raman spectrum of $CB_{11}H_{12}^-$ with the experimental room-temperature Raman spectrum of $Cs(CB_{11}H_{12})$ (left), and comparison of the experimental Raman spectra of $B_{12}H_{12}^{2-}$ [27] and $CB_{11}H_{12}^-$ (right).

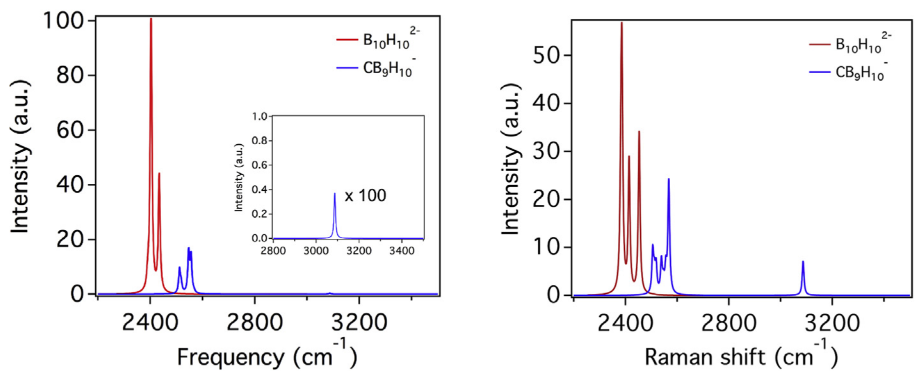

Fig. 5 – Comparison of the calculated anharmonic IR (left) and Raman (right) spectra of $CB_9H_{10}^-$ and $B_{10}H_{10}^{2-}$ (data for $B_{10}H_{10}^{2-}$ are from Ref. [27]).

this case, the inclusion of anharmonicity proves to be key to the accurate description of the B–H and C–H stretching modes, whose frequencies are otherwise noticeably overestimated.

As this can be inferred from the comparison in Fig. 5 of the IR and Raman spectra of $CB_9H_{10}^-$ and $B_{10}H_{10}^{2-}$, the B → C substitution in $B_{10}H_{10}^{2-}$ lead to similar trends in the vibrational spectra. The symmetry is lowered from D_{4d} to C_{4v}: the IR active modes transforming as E_1 and B_2 become E and A_1, respectively, and the Raman active modes transforming as E_3 become E while those of A_2 symmetry remain A_2 in C_{4v}.

For $B_{10}H_{10}^{2-}$ and $B_{12}H_{12}^{2-}$, the substitution of one boron atom by a carbon atom translate into a blue shift of the most intense bands of their Raman spectra between 550 cm^{-1} and 1200 cm^{-1} (see Supporting Information). Such a blue shift is also observed for the IR or Raman bands associated to the B–H stretching modes (see Fig. 5 and Supporting Information), and the C–H stretching modes are observed at 3071 and 3087 cm^{-1} for $CB_{11}H_{12}^-$ and $CB_9H_{10}^-$, respectively. The lengths of the B–H and C–H bonds in $CB_9H_{10}^-$, $B_{10}H_{10}^{2-}$, $CB_{11}H_{12}^-$ and $B_{12}H_{12}^{2-}$ as well as the associated stretching frequencies are summarized in Table 2.

The inspection of Table 2 shows that the B → C substitution in $B_{10}H_{10}^{2-}$ and in $B_{12}H_{12}^{2-}$ leads to a ~0.01 Å shortening of the B–H bonds, hence to a strengthening of these bonds, and concomitantly to a large increase of the stretching frequencies. One also notes that the C–H bond is predicted to be sligthy larger in $CB_{11}H_{12}^-$ than in $CB_9H_{10}^-$, which is the reverse of the order observed for the C–H stretching frequencies.

Table 2 – The B–H and C–H bond lengths and the associated anharmonic stretching frequencies for $CB_9H_{10}^-$, $B_{10}H^{2}{}_{0}^{-}$, $CB_{11}H_{12}^-$, and $B_{12}H^{2}{}_{2}^{-}$ (B3LYP-D2/cc-pVTZ results).

	r_{B-H} (Å)	ν_{B-H} (cm^{-1})	r_{C-H} (Å)	ν_{C-H} (cm^{-1})
$CB_9H_{10}^-$	1.186–1.190	2505–2560	1.078	3087
$CB_{11}H_{12}^-$	1.185–1.188	2510–2570	1.081	3071
$B_{10}H_{10}^{2-}$	1.201–1.205	2380–2450	–	–
$B_{12}H_{12}^{2-}$	1.198	2410–2470	–	–

Concluding remarks

We have performed a detailed DFT study of the vibrational spectroscopy properties of $Mg(B_3H_8)_2$, $CB_9H_{10}^-$ and $CB_{11}H_{12}^-$, with the inclusion of anharmonic effects. We have also measured the IR and Raman spectra of $CB_{11}H_{12}^-$ in $Cs(CB_{11}H_{12})$ and $B_{10}H_{10}^{2-}$ in $Na_2(B_{10}H_{10})$. A very satisfactory agreement has been observed between the calculated and experimental spectra. The results obtained for $Mg(B_3H_8)_2$ and $CB_{n-1}H_n^-$ ($n = 10$ and $n = 12$) have been compared to those previously reported for $B_3H_8^-$ and $B_nH_n^{2-}$ ($n = 10$ and $n = 12$), respectively [27]. For $B_3H_8^-$ and $Mg(B_3H_8)_2$, the comparative analysis helped evidence the influence of the binding to Mg^{2+} on both the structural and vibrational properties of $B_3H_8^-$. For $B_nH_n^{2-}$ ($n = 10$ or $n = 12$), the B → C substitution was shown to give rise to the shortening of the B–H bonds, which is accompanied by a large increase of the B–H stretching frequencies, and to the expected appearance of a C–H stretching band at 3071 cm^{-1} and at 3087 cm^{-1} for $CB_{11}H_{12}^-$ and $CB_9H_{10}^-$, respectively.

The vibrational frequencies reported in this study correspond to fundamental vibrational frequencies. Interestingly however, a preliminary analysis suggests that the overtones and combination bands cannot be fully neglected for $Mg(B_3H_8)_2$. The importance of the nonfundamental transitions in the vibrational spectra of boron-hydrogen species will be addressed in a future study.

Acknowledgment

This work was supported by the Swiss National Science Foundation (grant no. 200020_156681).

Appendix A. Supplementary data

Supplementary data related to this article can be found at http://dx.doi.org/10.1016/j.ijhydene.2017.03.044.

REFERENCES

[1] Yan Y, Remhof A, Rentsch D, Züttel A. The role of $MgB_{12}H_{12}$ in the hydrogen desorption process of $Mg(BH_4)_2$. Chem Commun 2015;51(4):700–2. http://dx.doi.org/10.1039/c4cc05266h.

[2] Liu Y, Giri S, Zhou J, Jena P. Intermediate phases during decomposition of metal borohydrides, $M(BH4)_n$ (M = Na, Mg, Y). J Phys Chem C 2014;118:28456. http://dx.doi.org/10.1021/jp509223d.

[3] Paskevicius M, Pitt MP, Webb CJ, Sheppard DA, Filsø U, Gray EM, et al. In-situ x-ray diffraction study of γ-$Mg(BH_4)_2$ decomposition. J Phys Chem C 2012;116(29):15231–40. http://dx.doi.org/10.1021/jp302898k.

[4] Zhang Y, Majzoub E, Ozoliņš V, Wolverton C. Theoretical prediction of metastable intermediates in the decomposition of $Mg(BH_4)_2$. J Phys Chem C 2012;116(19):10522–8. http://dx.doi.org/10.1021/jp302303z.

[5] Li H-W, Miwa K, Ohba N, Fujita T, Sato T, Yan Y, et al. Formation of an intermediate compound with a $B_{12}H_{12}$ cluster: experimental and theoretical studies on magnesium borohydride $Mg(BH_4)_2$. Nanotechnology 2009;20(20):204013. http://dx.doi.org/10.1088/0957-4484/20/20/204013.

[6] Hwang S-J, Bowman RC, Reiter JW, Rijssenbeek JW, Soloveichik GL, Zhao J-C, et al. NMR confirmation for formation of $[B_{12}H_{12}]^{2-}$ complexes during hydrogen desorption from metal borohydrides. J Phys Chem C 2008;112(9):3164–9. http://dx.doi.org/10.1021/jp710894t.

[7] Saldan I. Decomposition and formation of magnesium borohydride, Int. J Hydrogen Energy 2016;41(26):11201–24. http://dx.doi.org/10.1016/j.ijhydene.2016.05.062. http://www.sciencedirect.com/science/article/pii/S0360319916315026.

[8] Zavorotynska O, Deledda S, Hauback BC. Kinetics studies of the reversible partial decomposition reaction in $Mg(BH_4)_2$. Int J Hydrogen Energy 2016;41(23):9885–92. http://dx.doi.org/10.1016/j.ijhydene.2016.02.153. special Issue: 1st International Symposium on Materials for Energy Storage and Conversion (mESC-IS 2015), http://www.sciencedirect.com/science/article/pii/S0360319916308527.

[9] Tang WS, Matsuo M, Wu H, Stavila V, Zhou W, Talin AA, et al. Liquid-Like ionic conduction in solid lithium and sodium monocarba-closo-decaborates near or at room temperature. Adv Energy Mater 2016;6(8):1502237. http://dx.doi.org/10.1002/aenm.201502237.

[10] Wu H, Tang WS, Zhou W, Tarver JD, Stavila V, Brown CM, et al. The low-temperature structural behavior of sodium 1-carba-closo-decaborate: NaCB9H10. J Solid State Chem 2016;243:162–7. http://dx.doi.org/10.1016/j.jssc.2016.08.024.

[11] Tang WS, Unemoto A, Zhou W, Stavila V, Matsuo M, Wu H, et al. Unparalleled lithium and sodium superionic conduction in solid electrolytes with large monovalent cage-like anions. Energy Environ Sci 2015;8(12):3637–45. http://dx.doi.org/10.1039/c5ee02941d.

[12] Skripov AV, Skoryunov RV, Soloninin AV, Babanova OA, Tang WS, Stavila V, et al. Anion reorientations and cation diffusion in $LiCB_{11}H_{12}$ and $NaCB_{11}H_{12}$: ^{1}H, ^{7}Li, and ^{23}Na NMR studies. J Phys Chem C 2015;119:26912. http://dx.doi.org/10.1021/acs.jpcc.5b10055.

[13] Sharma M, Sethio D, D'Anna V, Hagemann H. Theoretical study of $B_{12}H_{12}^{2-}$ species. Int J Hydrogen Energy 2015;40(37):12721–6. http://dx.doi.org/10.1016/j.ijhydene.2015.07.125.

[14] Sharma M, Sethio D, D'Anna V, Fallas JC, Schouwink P, Černý R, et al. Isotope exchange reactions in $Ca(BH_4)_2$. J Phys Chem C 2015;119(1):29–32. http://dx.doi.org/10.1021/jp5082609.

[15] Łodziana Z, Błonski P, Yan Y, Rentsch D, Remhof A. NMR chemical shifts of ^{11}B in metal borohydrides from first-principle calculations. J Phys Chem C 2014;118(13):6594–603. http://dx.doi.org/10.1021/jp4120833.

[16] Meier P, Neff M, Rauhut G. Accurate vibrational frequencies of borane and its isotopologues. J Chem Theory Comput 2011;7(1):148–52. http://dx.doi.org/10.1021/ct1004752.

[17] Nguyen MT, Matus MH, Dixon DA. Heats of formation of boron hydride anions and dianions and their ammonium salts $[B_nH_m^{y-}][NH_4^+]_y$ with y = 1-2. Inorg Chem 2007;46(18):7561–70. http://dx.doi.org/10.1021/ic700941c.

[18] Tian AX. Ab initio and electron propagator theory study of boron hydrides. J Phys Chem A 2005;109:5471–80.

[19] McKee ML, Wang Z-X, von Ragué Schleyer P. Ab initio study of the hypercloso boron hydrides B_nH_n and $B_nH_n^-$. Exceptional stability of neutral $B_{13}H_{13}$. J Am Chem Soc 2000;122(19):4781–93. http://dx.doi.org/10.1021/ja994490a.

[20] Scott AP, Radom L. Harmonic vibrational frequencies: an evaluation of hartree-fock, møller-plesset, quadratic configuration interaction, density functional theory, and semiempirical scale factors. J Phys Chem 1996;100(41):16502–13. http://dx.doi.org/10.1021/jp960976r.

[21] Bühl M, Gauss J, Hofmann M, Schléyer P v R. Decisive electron correlation effects on computed boron-11 and carbon-13 NMR chemical shifts. Application of the GIAO-MP2 method to boranes and carbaboranes. J Am Chem Soc 1993;115(26):12385–90. http://dx.doi.org/10.1021/ja00079a020.

[22] Bühl M, Schléyer P v R. Application and evaluation of ab initio chemical shift calculations for boranes and carboranes. How reliable are "accurate" experimental structures? J Am Chem Soc 1992;114:477–91.

[23] Beaudet RA. In: Advances in boron and boranes. VCH; 1988. p. 417. Ch. 20.

[24] McKee ML, Lipscomb WN. Ab initio study of the transient boron hydrides B_3H_7, B_3H_9, B_4H_8, and B_4H_{12} and the fluxional anion $B_3H_8^-$. Inorg Chem 1982;21(7):2846–50. http://dx.doi.org/10.1021/ic00137a060.

[25] Todd LJ, Siedle AR. NMR studies of boranes, carboranes and hetero-atom boranes. Prog NMR Spectroscopy 1979;13:87–176.

[26] Wann DA, Lane PD, Robertson HE, Holub J, Hnyk D. Structures of, and related consequences of deprotonation on, two C_s-Symmetric *arachno* nine-vertex heteroboranes, 4,6-$X_2B_7H_9$ (X = CH_2; S) studied by gas electron diffraction/quantum chemical calculations and GIAO/NMR. Inorg Chem 2013;52(8):4502–8. http://dx.doi.org/10.1021/ic302776d. pMID: 23541164. arXiv.

[27] Sethio D, Lawson Daku LM, Hagemann H. A theoretical study of the spectroscopic properties of B_2H_6 and of a series of $B_xH_y^{z-}$ species (x = 1-12, y = 3-14, z = 0-2): from BH_3 to $B_{12}H_{12}^{2-}$. Int J Hydrogen Energy 2016;41(16):6814–24. http://dx.doi.org/10.1016/j.ijhydene.2016.02.121.

[28] Frisch MJ, Trucks GW, Schlegel HB, Scuseria GE, Robb MA, Cheeseman JR, et al. Gaussian 09 revision D.01. Wallingford CT: gaussian Inc; 2009.

[29] Gaussian NEWS, v. 5, no. 2, summer 1994, p. 2. "Becke3LYP Method References and General Citation Guidelines".

[30] Becke AD. Density-functional thermochemistry. III. The role of exact exchange. J Chem Phys 1993;98(7):5648–52. http://dx.doi.org/10.1063/1.464913. http://jcp.aip.org/resource/1/jcpsa6/v98/i7/p5648_s1.

[31] Grimme S. Semiempirical GGA-type density functional constructed with a long-range dispersion correction. J Comput Chem 2006;27:1787–99.

[32] Barone V. Vibrational zero-point energies and thermodynamic functions beyond the harmonic approximation. J Chem Phys 2004;120(7):3059–65. http://dx.doi.org/10.1063/1.1637580.

[33] Barone V. Anharmonic vibrational properties by a fully automated second-order perturbative approach. J Chem Phys 2005;122(1):014108. http://dx.doi.org/10.1063/1.1824881.
[34] Bloino J, Barone V. A second-order perturbation theory route to vibrational averages and transition properties of molecules: general formulation and application to infrared and vibrational circular dichroism spectroscopies. J Chem Phys 2012;136(12):124108. http://dx.doi.org/10.1063/1.3695210.
[35] Chong M, Karkamkar A, Autrey T, Orimo S-I, Jalisatgi S, Jensen CM. Reversible dehydrogenation of magnesium borohydride to magnesium triborane in the solid state under moderate conditions. Chem Commun 2011;47(4). http://dx.doi.org/10.1039/C0CC03461D. 1330–1332, 00033.
[36] Yan Y, Remhof A, Rentsch D, Lee Y-S, Cho YW, Züttel A. Is $Y_2(B_{12}H_{12})_3$ the main intermediate in the decomposition process of $Y(BH_4)_3$? Chem Commun 2013;49(45):5234–6.
[37] Chong M, Matsuo M, Orimo S-I, Autrey T, Jensen CM. Selective reversible hydrogenation of $Mg(B_3H_8)_2/MgH_2$ to $Mg(BH_4)_2$: pathway to reversible borane-based hydrogen storage? Inorg Chem 2015;54(8):4120–5. http://dx.doi.org/10.1021/acs.inorgchem.5b00373. http://dx.doi.org/10.1021/acs.inorgchem.5b00373.
[38] Olson JK, Boldyrev AI. Ab initio characterization of the flexural anion found in the reversible dehydrogenation. Comput Theor Chem 2011;967(1):1–4. http://dx.doi.org/10.1016/j.comptc.2011.04.011.